

AD-A240 806



2

EXPERIMENTAL INVESTIGATION INTO THE EFFECT
OF LONG TERM THERMAL ANNEALS ON THE
THERMOELECTRIC PROPERTIES OF SILICON
GERMANIUM-GALLIUM PHOSPHIDE

FINAL TECHNICAL REPORT

by

D.M. Rowe, D.Sc.

June, 1991



United States Army

EUROPEAN RESEARCH OFFICE OF THE U.S. ARMY

London, England

Contract Number DAJA45-89-C-0029

UNIVERSITY OF WALES COLLEGE OF CARDIFF

Approved for Public Release
Unlimited

Distribution Unlimited

91-11595



**EXPERIMENTAL INVESTIGATION INTO THE EFFECT
OF LONG TERM THERMAL ANNEALS ON THE
THERMOELECTRIC PROPERTIES OF SILICON
GERMANIUM-GALLIUM PHOSPHIDE**

FINAL TECHNICAL REPORT

by

D.M. Rowe, D.Sc.

June, 1991

United States Army

EUROPEAN RESEARCH OFFICE OF THE U.S. ARMY

London, England

Contract Number DAJA45-89-C-0029

UNIVERSITY OF WALES COLLEGE OF CARDIFF

Approved for Public Release

Distribution Unlimited

ABSTRACT

In this report is embodied the result of an experimental investigation into the effect of thermal anneals on the thermoelectric properties of n-type silicon germanium-gallium phosphide material.

The construction of apparatus for measuring the electrical conductivity, Seebeck coefficient and thermal diffusivity is described and their performance assessed. A variety of techniques are employed in an attempt to identify the mechanisms /agencies responsible for the reported enhanced thermoelectric properties of these materials after they have been subjected to high temperature thermal anneals.

The results confirm that improvements in the electrical power factor of silicon germanium-gallium phosphide accompanies high temperature thermal annealing. It has also been confirmed that this increase can be further increased by subjecting the material to a high-low-high temperature heating sequence. A change in the relative contributions of the electronic and lattice component to the thermal conductivity accompanies cyclic high temperature heat treatment, although the total thermal conductivity remains approximately constant.

A considerable effort was made to relate changes in the electrical properties with the material's morphology but obtaining a correlation between them proved elusive. However, the highest power factor obtained in this investigation corresponded to a morphology which consisted of the host matrix and a significant proportion of white phase.

The effect of high temperature heat treatment on the carrier scattering mechanisms provided a surprise. The results indicate that the electron scattering mechanism in these alloys is altered, the heat treatment being accompanied with an increase in the electron - phonon scattering contribution.

Finally, the work on the long term stability of the electrical power factor revealed that the enhancement which accompanies high temperature heat

treatment is unstable at device operating temperatures. The reported improvement in the thermoelectric figure of merit being almost totally lost after a relatively short period of high temperature heat treatment in air.



Accession For	
NTIS GRA&I	<input checked="" type="checkbox"/>
DTIC TAB	<input type="checkbox"/>
Unannounced	<input type="checkbox"/>
Justification	
By _____	
Distribution/ _____	
Availability Codes	
Dist	Avail and/or Special
A-1	

Contents

1. List of Figures
2. List of Tables
3. General Introduction
4. Objectives
5. Construction of Apparatus
 - (a) Introduction
 - (b) Electrical Resistivity and Seebeck Coefficient
 - (c) Thermal diffusivity
6. Materials
7. Experimental Procedures
 - (i) Thermal Cycling
 - (a) Introduction
 - (b) Measurements
 - (c) Results
 - (d) Discussion
 - (ii) Relationships between Thermoelectric Parameters and Morphology
 - (a) Introduction
 - (b) Measurements
 - (c) Results
 - (d) Discussion
 - (iii) Scattering Mechanisms
 - (a) Introduction
 - (b) Measurements
 - (c) Results
 - (d) Discussion
 - (iv) Thermal Stability of Enhanced Power Factor
 - (a) Introduction
 - (b) Measurements
 - (c) Results
 - (d) Discussion
8. General Conclusions
9. Acknowledgements
10. References

1. List of Figures

- Figure 1 Electrical Resistivity and Seebeck Coefficient Apparatus
- Figure 2 Schematic Thermal Diffusivity Apparatus
- Figure 3 Furnace Assembly
- Figure 4 Thermal Diffusivity Calibration Curve
- Figure 5 Thermal Conductivity vs Electrical Conductivity
- Figure 6 SEM showing surface of specimen Cla before heat treatment
- Figure 7 SEM showing surface of specimen Cla after 25 minutes heat treatment at 1500K
- Figure 8 SEM showing surface of specimen Cla after 4 hours, 45 minutes heat treatment at 1500K
- Figure 9 SEM showing surface of material before heat treatment
- Figure 10 SEM showing surface of material after heat treatment at 1470K for 5 minutes
- Figure 11 SEM showing surface of material after heat treatment at 1470K for 8 hours
- Figure 12 SEM showing surface of material after heat treatment at 1470K for 6 hours followed by slow cooling
- Figure 13 Electrical Resistivity vs temperature for specimen Bla
- Figure 14 Seebeck Coefficient vs temperature for specimen Bla
- Figure 15 Power Factor vs temperature for specimen Bla
- Figure 16 Electrical Properties of specimen Bla versus period. of heat treatment
- Figure 17 Seebeck Coefficient vs temperature for specimen Ala
- Figure 18 Electrical Resistivity vs temperature for specimen Ala
- Figure 19 Seebeck Coefficient vs log Temperature
- Figure 20 Log Electrical Conductivity vs log Temperature
- Figure 21 Power factor vs time; specimen at 973K
- Figure 22 Power factor vs time; specimen at 1273K

2. LIST OF TABLES

1. Thermoelectric parameters of G5 for high-low-high temperature heat treatment
2. A comparison of Electrical Properties before and after heat treatment
3. Values of the scattering parameters (q) before and after heat treatment

3. General Introduction

As part of an advanced thermoelectric materials development programme the Jet Propulsion Laboratory is investigating the preparation and properties of a number of semiconductor materials. Alloys based upon silicon germanium have been identified as a front runner material for use in the next generation of thermoelectric conversion systems for space applications. A concentrated effort has been maintained to increase the thermoelectric performance of these materials and improve their long term stability when operating at reactor powered device temperatures. The worth of a semiconductor in thermoelectric energy conversion is indicated by its figure of merit $Z = \alpha^2 \sigma / \lambda$ where α is the Seebeck coefficient σ the electrical conductivity and λ the thermal conductivity. The thermal conductivity consists mainly of two components λ_L , a contribution due to the lattice and a contribution λ_c due to the charge carriers. Generally, in thermoelectric semiconductors the lattice component is the major contribution. Significant reductions in the lattice thermal conductivity of these materials have been achieved by employing small grain size (1) and through the introduction of III-V additives such as gallium phosphide (2). However, any beneficial reduction in the thermal conductivity has been largely offset by an increase in the electrical resistivity.

It has been reported that the thermoelectric figure of merit and in particular the electrical power factor of silicon germanium-gallium phosphide can be significantly improved by subjecting this material to high temperature thermal anneals (3). Researchers at the Jet Propulsion Laboratory attribute this improvement as being possibly due to an increase in dopant solubility.

The behaviour of dopant solubility in n-type SiGe and in p-type SiGe which accompanies various heat treatments has been investigated thoroughly (4, 5) and a model developed which enabled accurate predictions to be made of the long term behaviour of the materials in actual device applications. Preliminary results of a theoretical investigation of the thermoelectric properties of silicon germanium-gallium phosphide material, undertaken at Cardiff (U.S. Army Contract DAJA45-88-M-0424) indicated that a simple increase in dopant solubility due to the presence of gallium phosphide is unlikely to explain the magnitude of the reported improvement in material performance. The situation is complicated and

involves the consideration of SiGe-GaP as a different material rather than SiGe with small amounts of GaP as an additive. Identifying the mechanisms/agencies responsible for the improved thermoelectric behaviour of these modified materials is evidently relevant to a material development programme as is their behaviour when subjected for long periods of time at device operating temperatures. In this programme of research a number of procedures have been employed in an attempt to obtain this information.

4. Objectives

There were five main objectives to the programme of research.

1. Construct apparatus for the measurement of Seebeck coefficient electrical resistivity and thermal diffusivity.
2. Confirm the reported improvement in electrical power factor which accompanies thermal cycling.
3. Investigate relationships between thermoelectric parameters and material morphology.
4. Investigate the effect of heat treatment on the scattering parameter.
5. Investigate the thermal stability of the enhanced power factor.

5. Construction of Apparatus

(a) Introduction

Apparatus was required to subject the materials under investigation to a variety of high temperature heat treatment procedures and monitor the behaviour of their electrical power factor and the figure of merit. To meet this requirement several temperature controlled heat treatment furnaces were obtained. Apparatus was also constructed to measure the Seebeck coefficient, electrical conductivity and thermal diffusivity over the temperature range from room temperature to about 900K. A wide range of techniques were also employed in assessing changes in material morphology.

(b) Electrical Resistivity and Seebeck coefficient

The apparatus used is shown schematically in Figure 1. Based upon a well established method (6) ingot shaped specimens (Typical dimensions 5.5 x 2.5 x 2.0mm) are held between two spring loaded cylindrical copper blocks. Molybdenum foils inserted between the sample and the block minimise contamination of the specimen by the copper. Non inductive heaters are wound around electrically insulating ceramic sleeves which fit snugly over the copper blocks and are cemented in position with thermal conducting paste. A controllable small temperature gradient (a few degrees) is maintained across the sample by adjusting the power through these heaters. Two thermocouples are wedged with graphite into small holes a measured distance apart and cut ultrasonically into the sample. The selection of thermocouple material is a choice between platinum-rhodium and chromel-alumel, the two most common types of thermocouples used over this temperature range. Platinum-rhodium thermocouples generate reproducible output voltages and almost matching thermocouples can be fabricated relatively easily. However, the output voltages are small and the thermocouples react with silicon at high temperatures. On the other hand it was very difficult to make matching thermocouples with chromel-alumel, and in addition they cannot be used in vacuum for long periods and become unstable at high temperatures (an upper operating temperature of about 850K). Chromel-alumel however, produces relatively large voltages which facilitates direct coupling to a chart recorder; this was an important consideration and resulted in their choice as a thermocouple material. The Seebeck coefficient of the specimen is obtained from the temperature difference between the thermocouples and the corresponding Seebeck voltage; the electrical resistivity can be derived from the voltage drop between similar legs of the thermocouple when a current passes through the specimen under isothermal conditions. The limit of the reproducibility and accuracy of measurement of electrical resistivity was largely due to uncertainties associated with the electrical separation of the contact probes. Estimated error in the Seebeck coefficient and electrical resistivity measurements were $\pm 3\%$ and $\pm 4\%$ respectively and about $\pm 6\%$ in the electrical power factor.

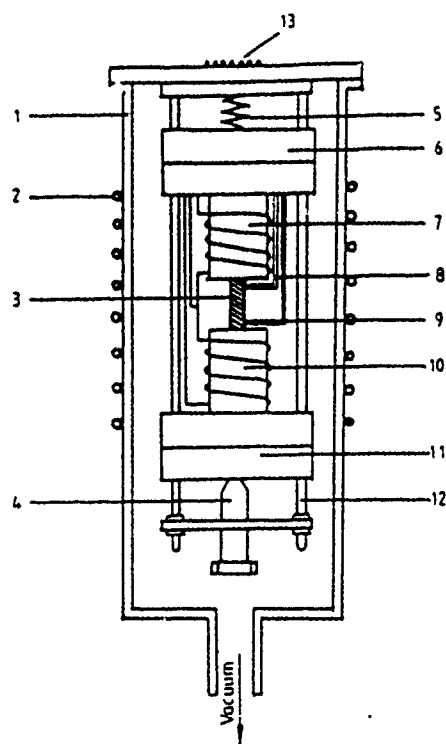


Figure 1. Apparatus for measurement of Seebeck coefficient and electrical resistivity (not to scale). 1, vacuum vessel; 2, cooling coil; 3, specimen; 4, pressure screw; 5, pressure spring; 6, 11, heater supports; 7, 10, heaters; 8, 9, thermocouples; 12, stainless steel rods; 13, leads feedthrough.

Figure 1 Electrical Resistivity and Seebeck Coefficient Apparatus

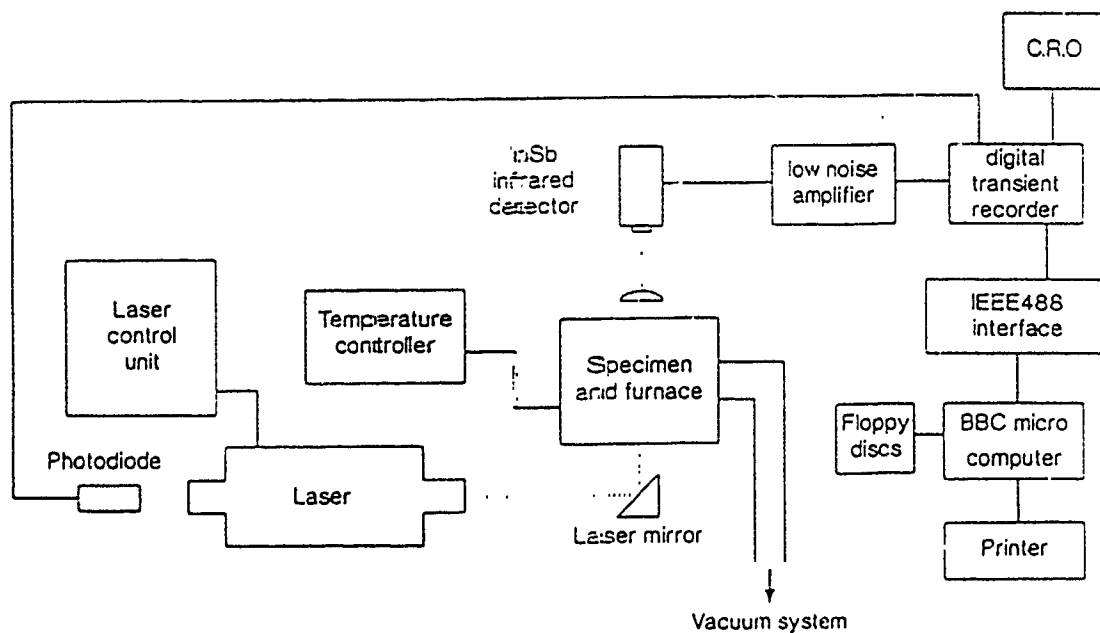


Figure 2 Schematic Thermal Diffusivity Apparatus

(c) Thermal Diffusivity

A schematic of the thermal diffusivity measuring apparatus is shown in Figure 2. The heat pulse is provided by a neodymium glass laser with a maximum output of 16J per flash and a pulse duration of 1 msec. The laser is mounted on an optical bench which also provides support for the furnace.

The furnace consists of a 30mm outside diameter ceramtec tube, 120mm long and wound with a nichrome wire resistance heater. This is enclosed within a second pyrophyllite ceramic sheath and mounted vertically. A graphite tube fits inside the heater and serves to support the specimen holder horizontally. The latter consists of a ceramtec disc, 13mm diameter and 5mm thick with a recess to locate the specimen centrally as indicated in Figure 3. A 5mm diameter hole beneath the specimen exposes its surface to the laser radiation after it has been reflected through 90 degrees. Infrared radiation from the rear surface of the specimen is focussed by a plano-convex CaF_2 lens onto a InSb infrared detector. A screw type mounting facility focussing on the detector system. The detector is electrically insulated from the furnace to avoid earthing loops.

Output from the detector is increased by a two stage low noise amplifier before feeding into a digital storage system. The input stage facilities offsetting of unwanted background signals at higher temperatures and provides correct impedance matching and biasing of the detector. Adjustable gain and further bucking off is provided by the second stage. Samples of the signal are taken at time intervals depending upon the sampling rate. This can be varied in 15 ranges from 5Hz to 200Hz. A fast response photodiode switch ensures synchronisation of the recorder with the laser flash while a storage oscilloscope provides visual display of the temperature transient before transferring to the computer for analysis.

The performance of the apparatus is illustrated by measurements made on a reference material, Armco iron Figure 4 shows the experimental data indicated by solid points, the solid curve represents accepted values obtained by other researchers (7,8). The apparatus provided data up to a temperature of 1000K which deviated by less than 4% from accepted

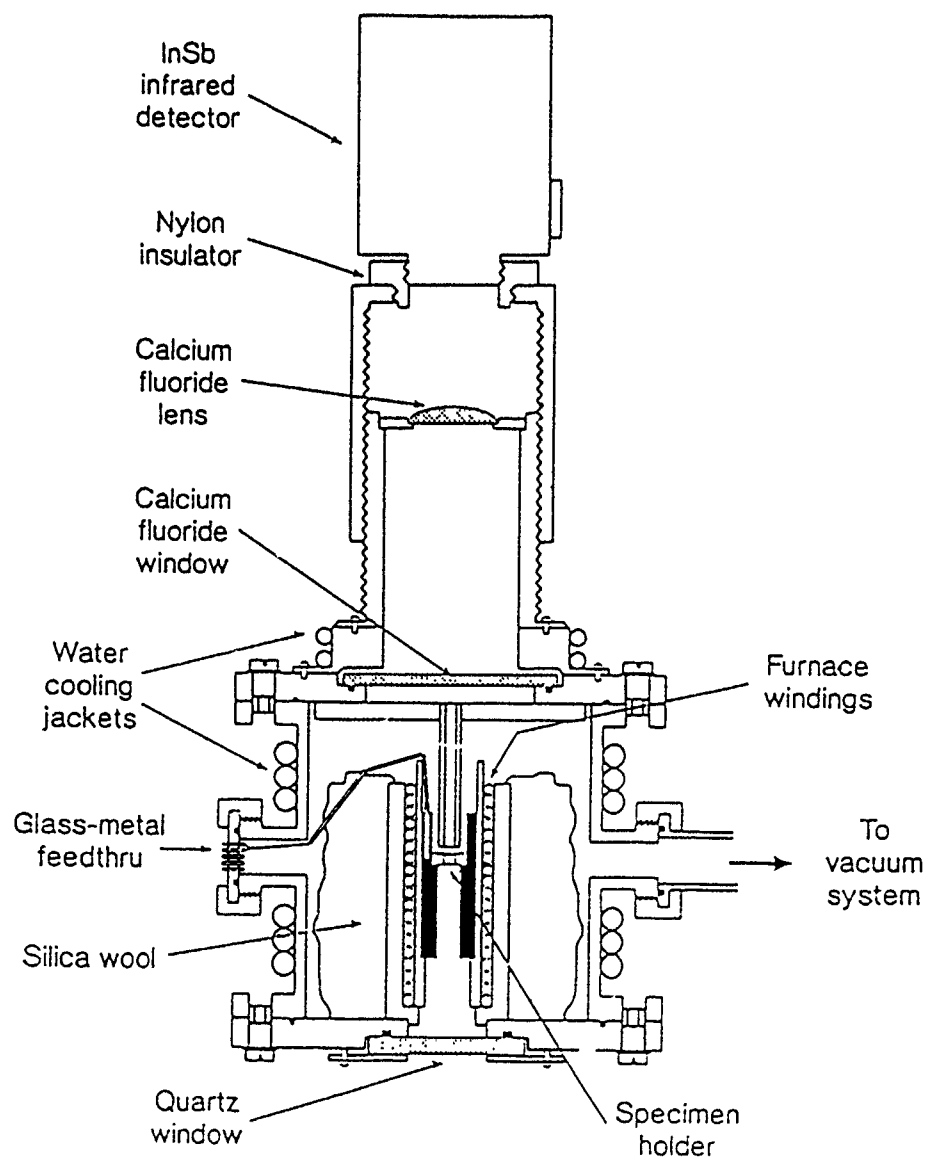


Figure 3 Furnace Assembly

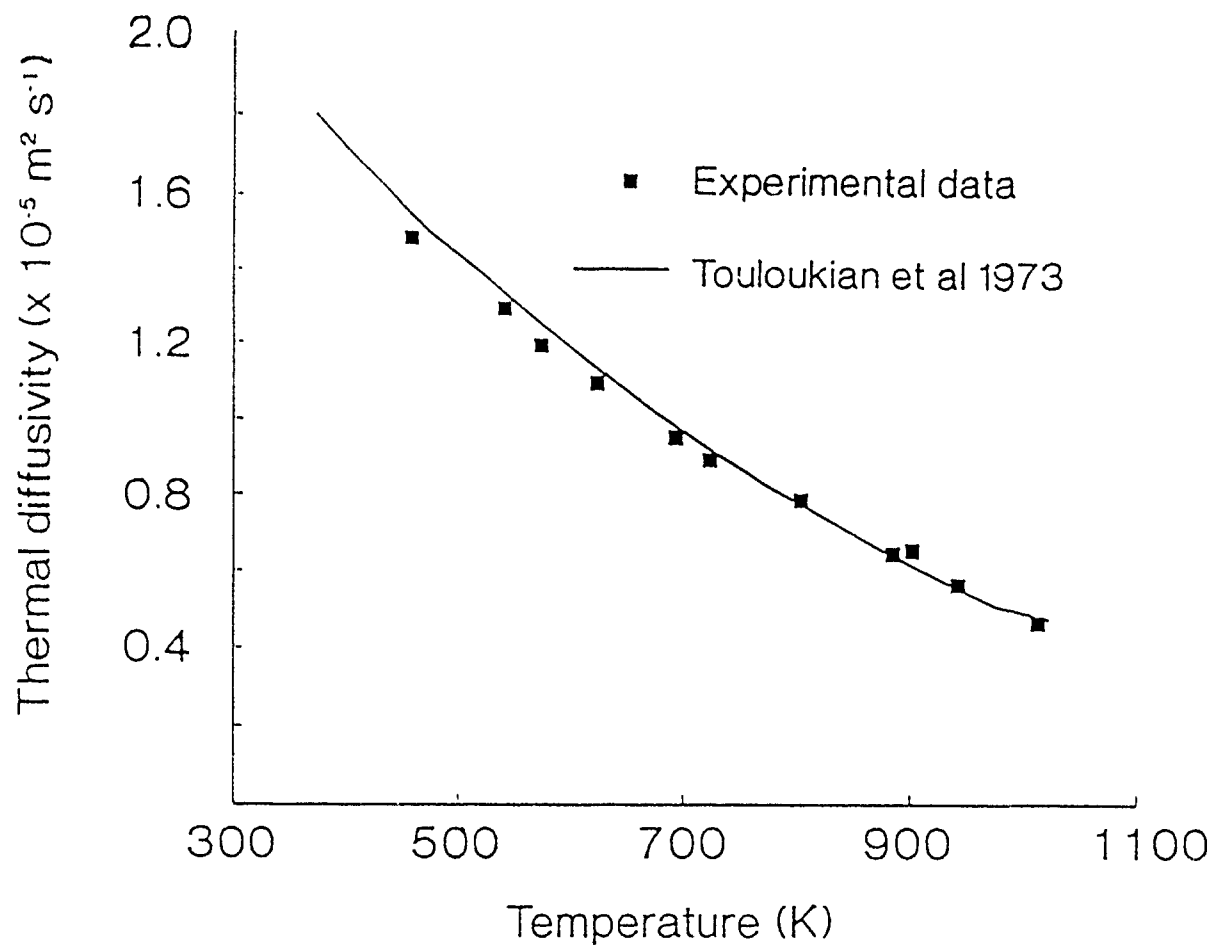


Figure 4 Thermal Diffusivity Calibration Curve

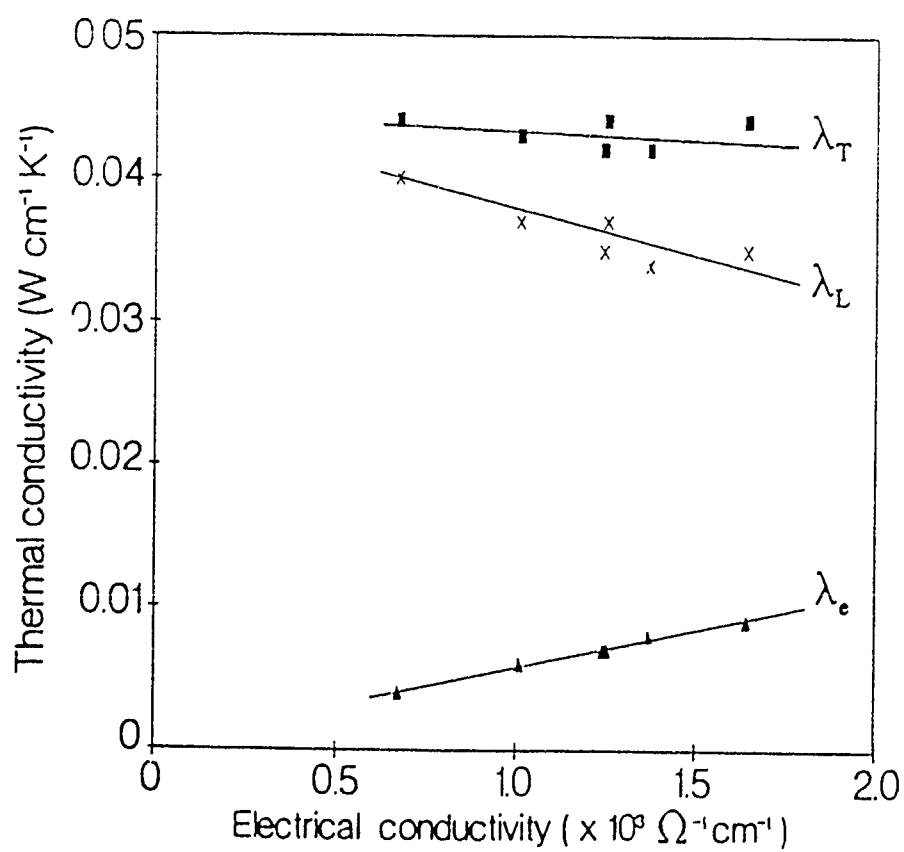


Figure 5 Thermal Conductivity vs Electrical Conductivity

values. Reproducibility of data at 1000K was a better than 3%. At temperatures below 400K data reproducibility using the InSb detector was poor and an intrinsic type-K thermocouple was used.

The thermal conductivity can be obtained from the measured thermal diffusivity using the relationship $\lambda = C_p \lambda'$

Where C is the specific heat, ρ the density and λ' the thermal diffusivity.

6. Materials

The material used in this programme of research was obtained from the Jet Propulsion Laboratory, Pasadena, U.S.A. in the form of small cylindrical pellets. Reference data indicated that the alloy composition was about $\text{Si}_{80}\text{Ge}_{20}$ with about 2% gallium phosphide. The high density pellets (about 3.0g cm^{-3}) were sliced with a diamond saw. Various geometries required for different transport property measurement were cut using an ultrasonic cutter.

7. Experimental Procedures

(i) The effects of thermal cycling.

(a) Introduction

Significant increases in the electrical power factor of silicon germanium-gallium phosphide alloys have been obtained by heat treatment at high temperatures (3) and similar results have been achieved by subjecting the material to cyclic heat treatments (9). Although the total thermal conductivity is reported to remain almost constant no data is available in the literature relating to the behaviour of the two main components of the thermal conductivity has been reported. Such information is helpful in any attempt to identify agencies/mechanism which are responsible for the improvement in the material's performance.

(b) Measurements

Two disk shaped specimens (identified as G5 and C1a), 6.5mm diameter and 1-1.5mm thick were used for thermal diffusivity measurements. The specimens were polished using a range of abrasive papers to obtain parallel faces. Both specimens were heat treated in air at 1500K for 10, 20 and 60 minutes, and finally heat treated at 153K for 180 minutes. The other specimen (G5) was heat treated in air for 4 hours at 1500K, and 975K. Each heat treatment was followed by air quenching to room temperature. Prior to measurement the surfaces were etched with HF (40%), polished and cleaned using methanol. Thermal diffusivity of the specimens was measured using a laser flash apparatus described in Section 5c

Electrical measurements were made using a conventional four probe technique (10) accuracy is about 2%. The Seebeck coefficient was measured using a hot probe (11) accuracy 3%. Both electrical and thermal diffusivity measurements were carried out at room temperature.

(c) Results

The effect of the cyclic heat treatment on the Seebeck coefficient, electrical conductivity and thermal conductivity of specimen G5 are shown in Table 1.

TABLE 1
THERMOELECTRIC PARAMETERS OF SPECIMEN
G5 FOR HIGH-LOW-HIGH TEMPERATURE
HEAT TREATMENT

Heat treatment	α ($\times 10^{-6}$ V/K)	σ ($\times 10^3 \Omega^{-1} \text{cm}^{-1}$)	λ ($\text{Wcm}^{-1} \text{K}^{-1}$)
BEFORE	117	0.79	0.045
H1(1500K 4h)	83	1.43	0.041
H2(975K 4h)	105	1.08	0.042
H3(1500K 4h)	85	1.45	0.042

The initial heat treatment at 1500K for 4 hours (H1), resulted in an increase in electrical conductivity accompanied by a less significant decrease in the Seebeck coefficient. In contrast the second heat treatment H2) at a lower temperature (975K) produced a reduction in electrical conductivity and an increase Seebeck coefficient. Finally heat treatment at 1500K (H3) resulted in the electrical conductivity increasing slightly above its value after the initial high temperature heat treatment. This increase was accompanied by a slightly increased Seebeck coefficient compared with the initial heat treatment (H1). There appears to be no significant change in the total thermal conductivity of silicon germanium-gallium phosphide alloys following cyclic heat treatment. The increase in the electrical conductivity suggests that the charge carrier contribution (λ_e) is increasing. To confirm this specimen C1a was subjected to short successive heat treatments of 5, 10, 20 and 60 minutes at 1500K and 180 minutes at 1530K. At each stage the electrical conductivity and total thermal conductivity was obtained. Changes in thermal conductivity with electrical conductivity are shown in Figure 5. The total thermal conductivity (λ) was obtained from laser pulse thermal diffusivity measurements. The electronic component was estimated using $\lambda_e = \frac{1}{2} \sigma T$ where the Lorenz number ($\frac{1}{2}$) is assumed to remain constant and was taken as $1.90 \times 10^{-4} \text{ V}^2 \text{ K}^{-2}$. The lattice thermal conductivity is obtained from the relationship $\lambda_L = \lambda - \lambda_e$.

(d) Discussion

It is apparent from the investigation that the electronic thermal conductivity increases with increasing electrical conductivity and is accompanied by a corresponding decrease in the lattice thermal conductivity. The total thermal conductivity remains essentially unchanged, which suggests that the high temperature heat treatment of these alloys affects the relative contribution of both lattice and electronic components. As a result λ_e is significantly increased after heat treatment from about 10% to 25%, which favours an improvement in the figure of merit Z (12). The increase in λ_e with electrical conductivity is to be expected, however the decrease in λ_L requires some explanation. A substantial reduction in the lattice thermal conductivity of SiGe alloys can be achieved by the use of fine grain size material and by the introduction of III-V additives such as GaP as indicated in section 3. In fine grained hot pressed SiGe-GaP alloys an increase in electrical conductivity,

partially attributed to an increase in carrier concentration will be accompanied by an increase in phonon electron scattering. A similar result has been observed in SiGe alloys (13) and a theoretical consideration has been published recently (14).

Scanning electron microscopy (SEM) was employed to assist in further identification of the microstructure which may be responsible for the decreases in λ_L . Figures 6-8 illustrate the changes in microstructure before and after heat treatment. Prior to heat treatment two phases were identified using SEM, a host matrix and "black phase" ESCA (Electron Spectroscopy for Chemical Analysis). Examinations indicate the host matrix composition is about 80% Si-20%Ge while the black phase is silicon rich with 95% Si-5%Ge. After a short heat treatment at high temperature the amount of "black phase" decreases and a "white phase" appears as shown in Figure 7. The composition of this "white phase" was found to be about 60%Si-40%Ge. Further heat treatment reduced the "black phase" until after 3 hours it had completely disappeared and only "white phase" and host matrix are observed. After heat treatment the composition of the host matrix was found to be 85%Si-15%Ge.

It is well understood that the thermal conductivity of SiGe alloys changes with alloy composition, the lowest value is achieved with a composition of 60%Si-40%Ge (15). Before heat treatment the black phase accounts for approximately 10%-15% of the entire volume, that is at least 10% of the specimen has a very high thermal conductivity. After heat treatment the high thermal conductivity region is reduced and replaced by a white phase of considerably lower thermal conductivity. Of course the thermal conductivity of the host matrix has been increased slightly with a change in the silicon content although this increase will most probably be dominated by the reduction in lattice thermal conductivity which accompanies the disappearance of the black phase. Consequently microstructural changes introduced by high temperature heat treatment results in an overall decrease in the lattice thermal conductivity of silicon germanium-gallium phosphide.



Figure 6. SEM showing surface of specimen C1a before heat treatment



Figure 7. SEM showing surface of specimen C1a after 25 minutes heat treatment at 1500 K



Figure 8. SEM showing surface of specimen C1a after 4hrs 45 min heat treatment over 1500 K

(ii) Relationships Between Thermoelectric Parameters and Material Morphology

(a) Introduction

The observation that the reduction in the lattice component of the thermal conductivity appeared to be associated with changes in the morphology of the material and in particular with the replacement of a high thermal conductivity black phase with a lower thermal conductivity white phase lead to the following work. The objective was to attempt to relate the effect of high temperature heat treatment on the electrical properties to changes in morphology.

(b) Measurements

Two ingot shaped specimens of dimensions of 2x2x10 mm and identified as Ala and Bla were cut from the pressed material. Specimen Bla was heat treated at 1470K for periods of 5, 10, 20, 40, 80 minutes, 7 hrs and 50 hrs. Heat treatment was carried out in air and followed by air quenching to room temperature. Prior to morphological examination and electrical property measurement, the specimen was etched with HF(40%) to remove the oxide layer formed on the surface during heat treatment, then polished and cleaned with methanol. Specimen Ala was used to investigate the relationship between the white phase and the electrical properties. Towards this end it was subjected to a high temperature heat treatment at 1470K and followed by a low temperature heat treatment at 970K. Both heat treatments were carried out in air for 8 hours then air quenched. Two other specimens A2i and A2j were used to compare the changes in morphology and electrical properties which accompany quenching and slow cooling. Specimen A2i was heat treated at 1470K for 6 hours then quenched, while specimen A2j was subjected to the same heat treatment but cooled slowly (10K/min.).

Morphological changes of the specimen before and after heat treatment were examined by SEM and the composition changes were semi-quantitatively determined using ESCA. Electrical resistivity and Seebeck coefficient measurements as a function of temperature were made using apparatus described in section 5b. Electrical resistivity measurements

for specimen A2i and A2j were made only at room temperature using a conventional four probe technique (10) and the Seebeck coefficient using a hot probe method (11).

(c) Results

The morphological changes which accompany different heat treatments are shown in Figures 9-12. Prior to heat treatment SEM examination revealed that the material consists of two phases, a host matrix and a black phase (Figure 9). ESCA examination indicated that the composition of the host matrix is about 80%Si-20%Ge with approximately 1% GaP while the black phase is silicon rich with a composition of about 95%Si-5%Ge. After subjecting the material to high temperature heat treatment for 5 minutes a white phase appears as shown in Figure 10. The composition of the white phase is about 60%Si-35%Ge with more than 3% GaP. The proportion of the black phase decreases with an increase in the period of heat treatment and completely disappears after around 4 hours of heat treatment as shown in Figure 11. The proportion of white phase can be reduced by slowly cooling the material (10K/min) to room temperature (Figure 12). Changes in the electrical resistivity, Seebeck coefficient and power factor of specimen B1a which accompany different heat treatments are displayed as a function of temperature in Figures 13,14 and 15. A substantial reduction in the electrical properties occurs during the first fifteen minutes of heat treatment. A less significant reduction in these properties accompanies further heat treatment with a subtle difference observed between the decrease in the Seebeck coefficient compared with the electrical resistivity as shown in Figure 16.

The effect of different cooling rates on the morphology are illustrated with reference to Figures 11 and 12. The morphology of specimens A2i after six hours of heat treatment followed by quenching was similar to Figure 11, while the morphology of specimen A2j after six hours of heat treatment followed by a slow cool is shown in Figure 12. The electrical properties of both specimens measured before and after heat treatment are collected in Table 2.

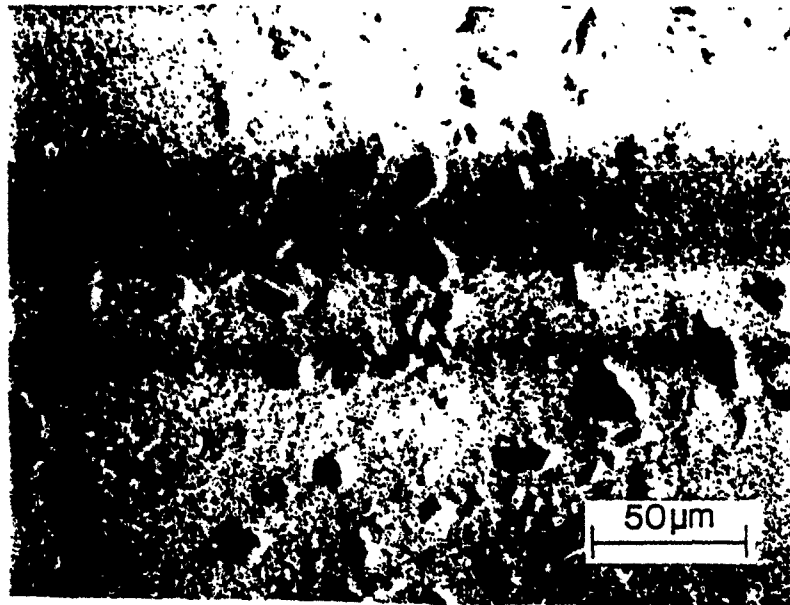


Figure 9 SEM showing surface of material before heat treatment

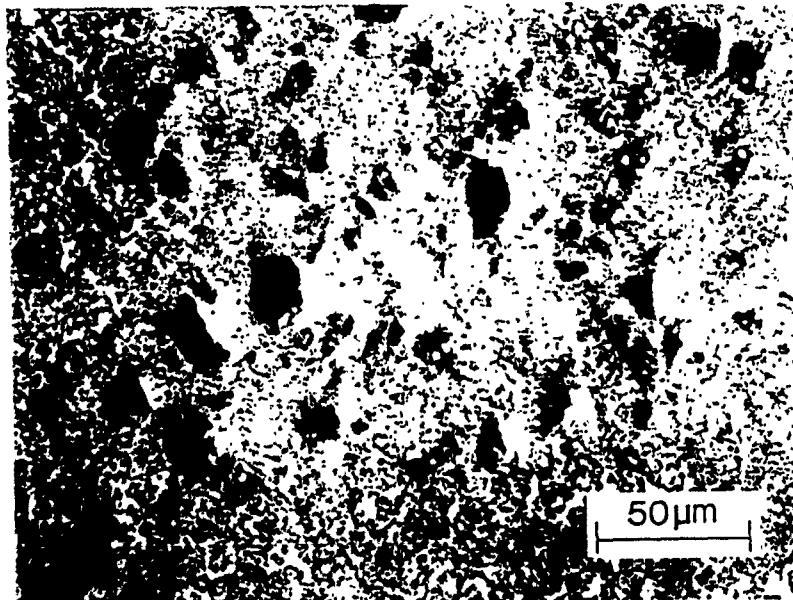


Figure 10 SEM showing surface of material after heat treatment at 1470K for 5 minutes



Figure 11 SEM showing surface of material after heat treatment at 1470K for 8 hours

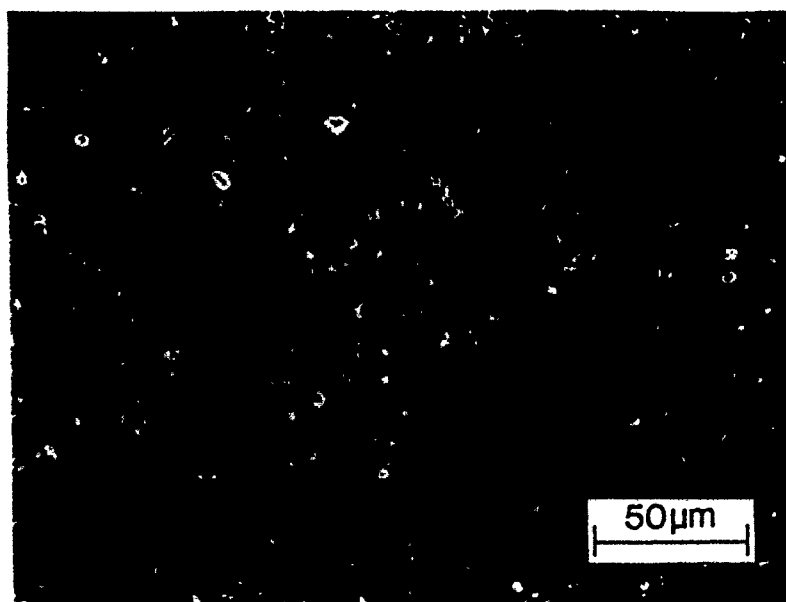


Figure 12 SEM showing surface of material after heat treatment at 1470K for 6 hours followed by slow cooling

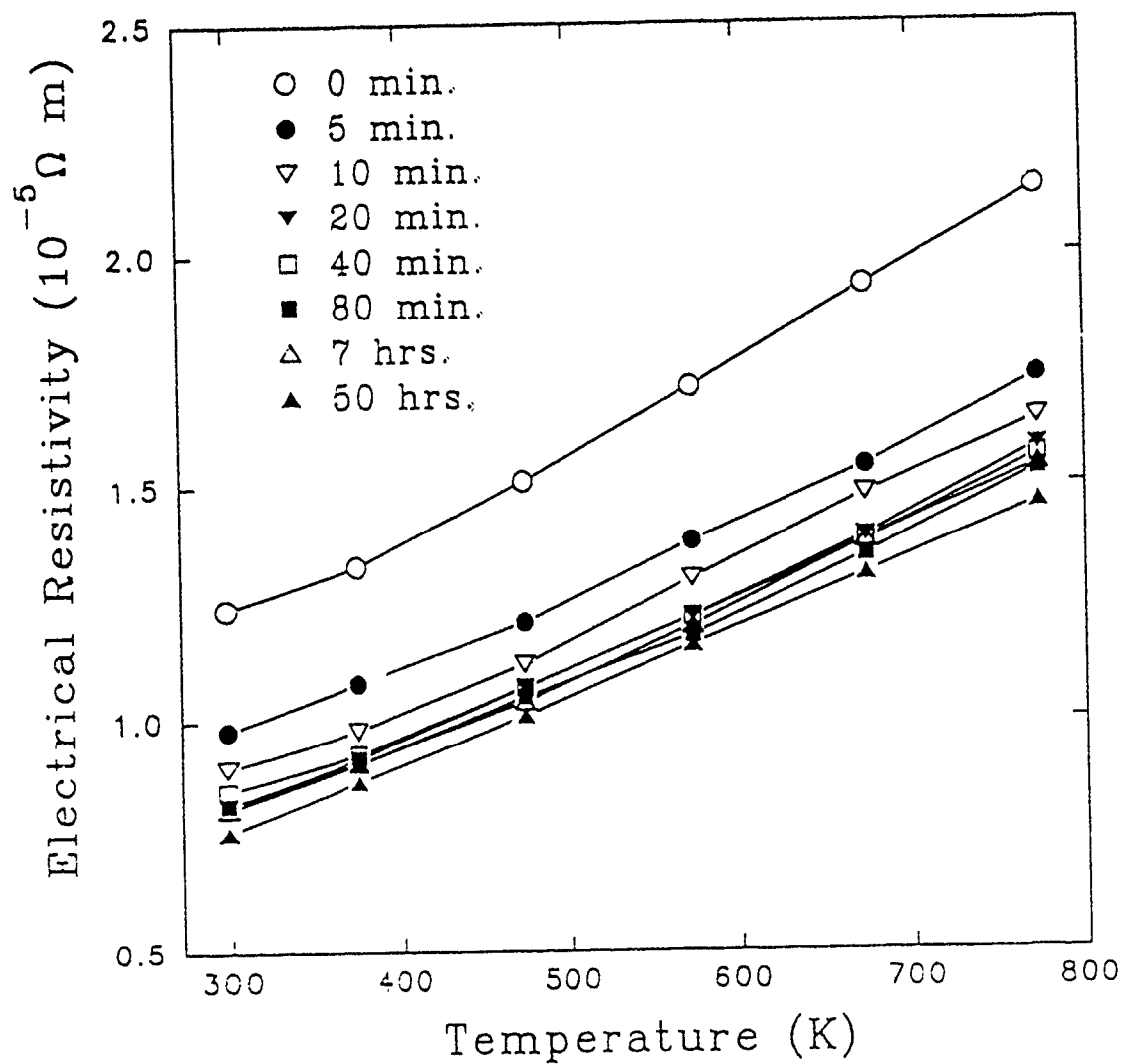


Figure 13 Electrical Resistivity vs temperature for specimen Bla

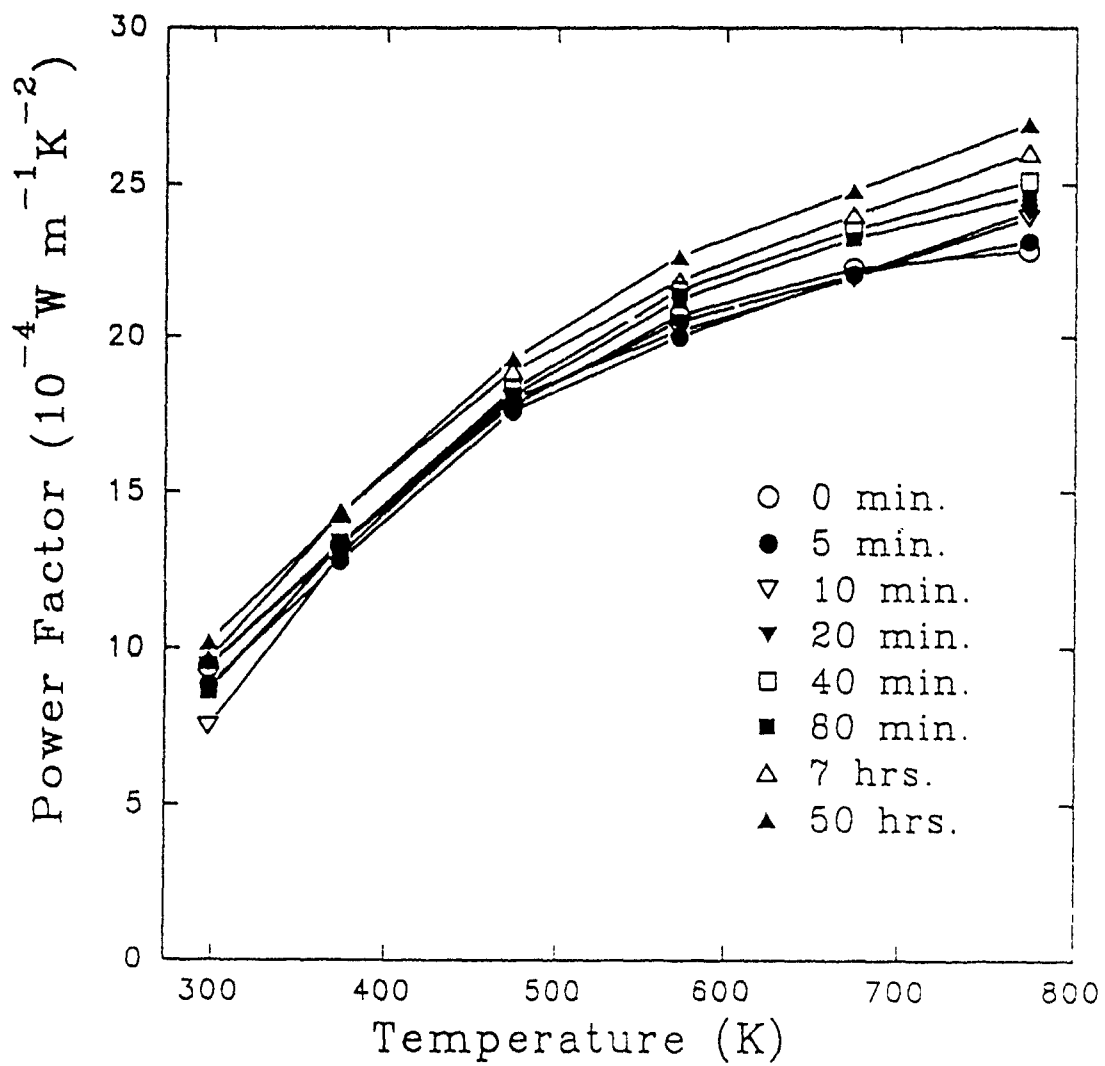


Figure 14 Seebeck Coefficient vs temperature for specimen Bla

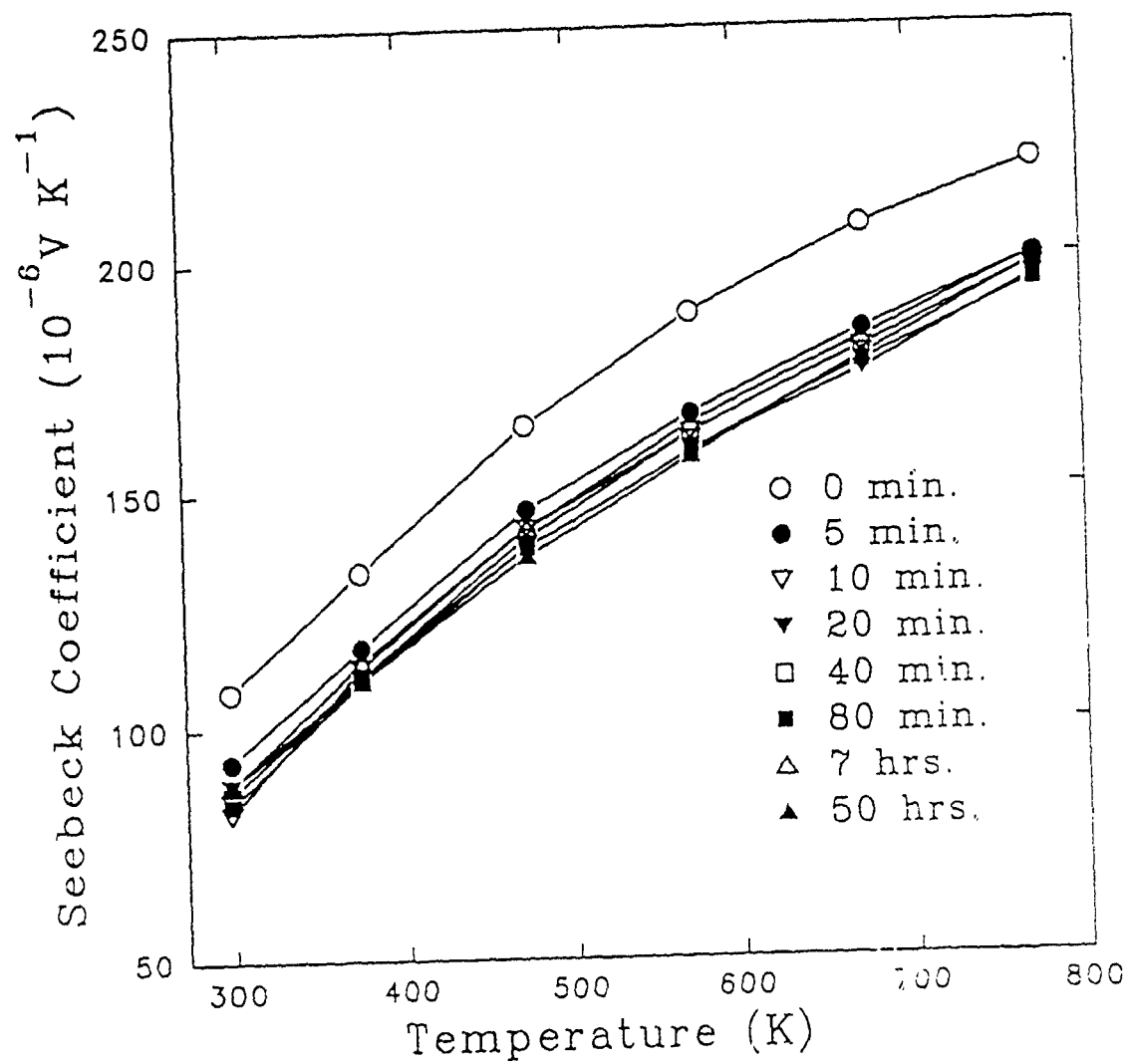


Figure 15 Power Factor vs temperature for specimen Bla

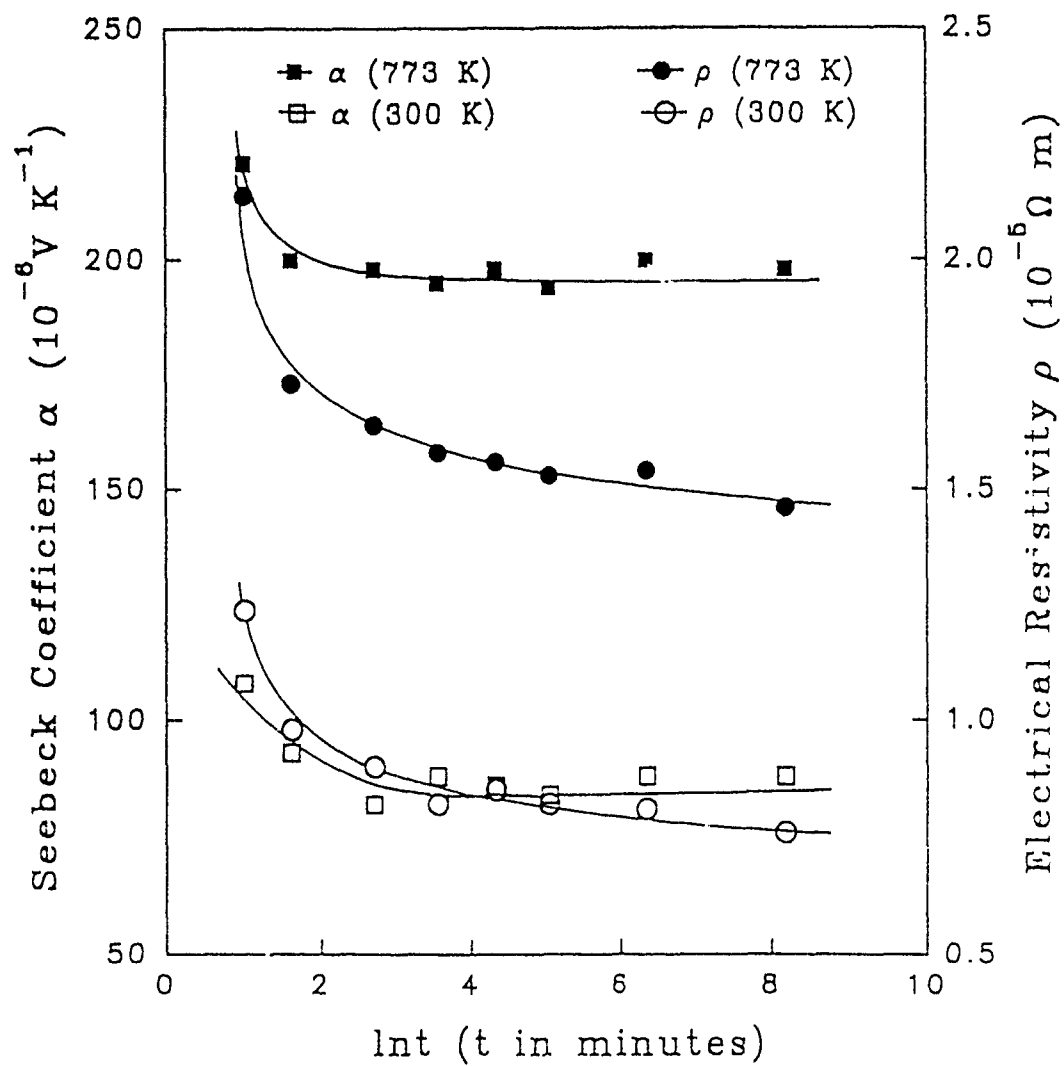


Figure 16 Electrical Properties of specimen Bla versus period. of heat treatment

TABLE 2

<u>A COMPARISON OF ELECTRICAL PROPERTIES</u>				
Specimens	Heat-treatment	$\alpha(*10^{-6}V/K)$	$\rho(*10^{-5}\Omega\ m)$	$\alpha^2\rho(*10^{-4}Wm^{-1}K^{-2})$
A2i	BHT	120	2.24	6.43
	HT6Q	83	0.78	8.83
A2j	BHT	121	2.28	6.42
	HT6S	92	1.14	7.42

BHT - Before heat treatment; HT6S - Heat treatment for 6 hours

followed by slow cooling; HT6Q - Heat treatment for 6 hours followed by quenching in air.

The morphology of Ala after its initial heat treatment at high temperature is also very similar to Figure 11. No significant change in the morphology accompanied heat treatment at a lower temperature although the Seebeck coefficient and electrical resistivity was altered significantly as displayed in Figures 17 and 18.

(d) Discussion

Silicon germanium gallium phosphide alloys exhibit different morphologies depending upon the temperature of heat treatment, the period of heat treatment and the rate at which the material is cooled. Four different morphologies have been observed as shown in Figures 9-12. The disappearance of the black phase after around 4 hours of heat treatment is irreversible. However, changes in the white phase is reversible. The proportion of white phase is significantly reduced if the high temperature heat treatment is followed by cooling the material to room temperature. Quenching the material after further high temperature heat treatment results in a material with a significant proportion of white phase. Comparing the material's morphology with the electrical properties indicated that the highest power factor corresponded to a morphology which consists of host matrix and a significant white phase.

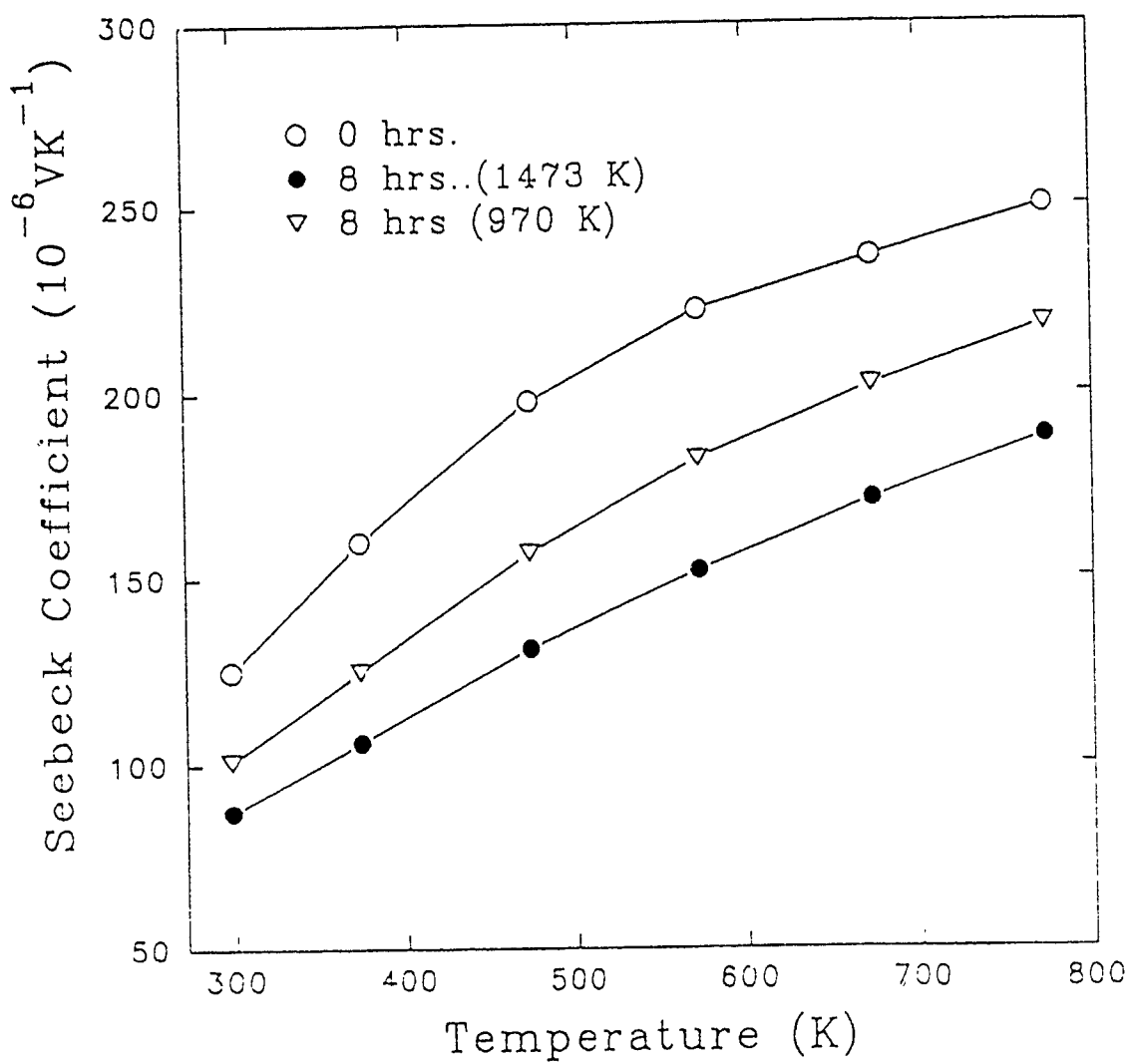


Figure 17 Seebeck Coefficient vs temperature for specimen Ala

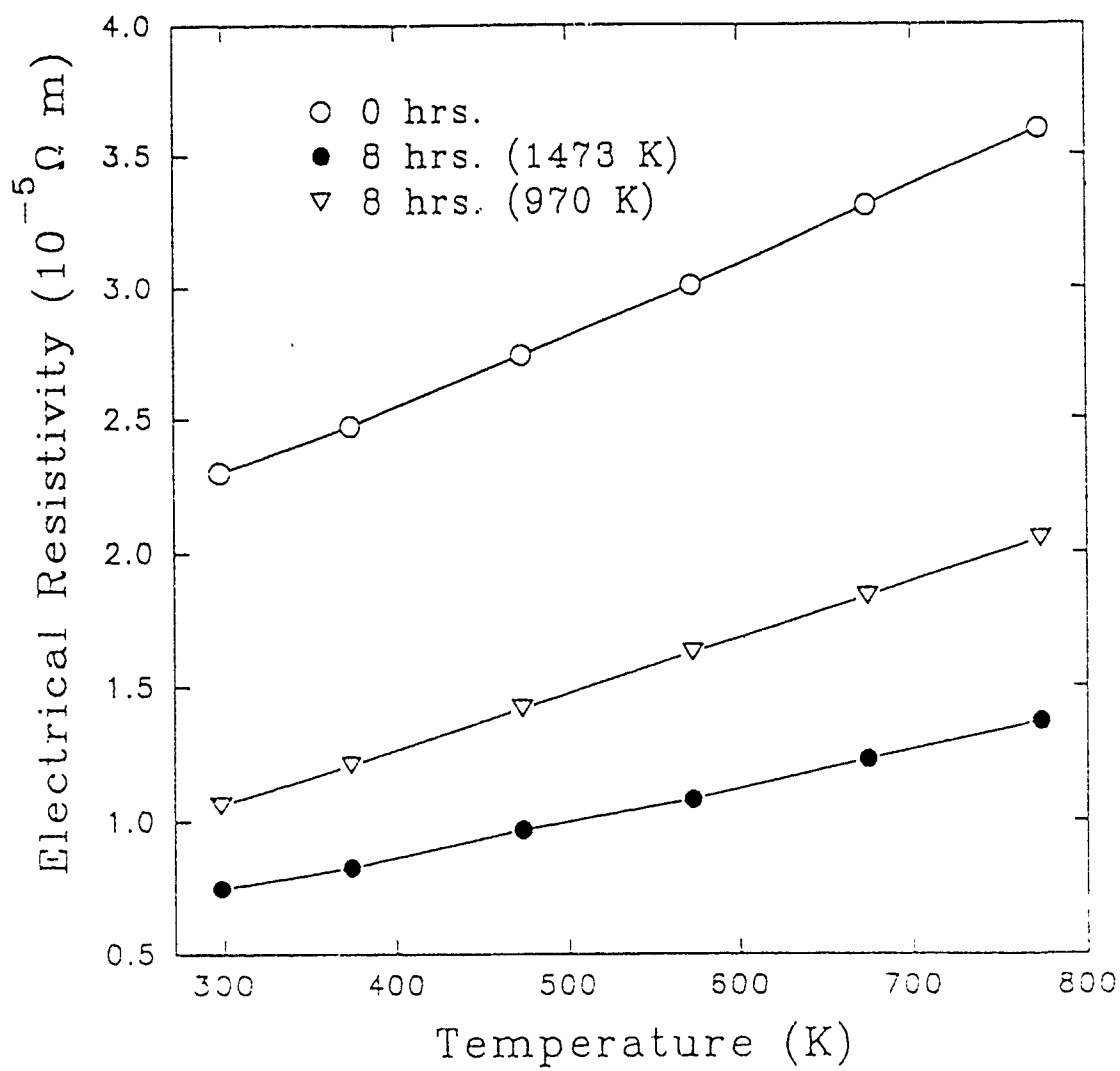


Figure 18 Electrical Resistivity vs temperature for specimen Ala

The measurements indicate that the electrical power factor increases with period of heat treatment. Although the electrical resistivity and the Seebeck coefficient change very significantly following a short period of heat treatment (<15 mins) the combined effect results in no improvement in the electrical power factor. An increase in the power factor accompanies relatively long periods of heat treatment and is due to a subtle difference in the behaviour of the electrical resistivity and Seebeck coefficient. As shown in Figure 16 the reduction in the electrical resistivity continues, albeit less pronounced, while the Seebeck coefficient remains essentially constant.

Although substantial changes in morphology and electrical properties accompany high temperature heat treatment, establishing any relationship between them has proved elusive. Results obtained to date indicate that neither the black phase nor the white phase play an important part in modifying the electrical properties. The electrical properties change substantially during the first fifteen minutes of heat treatment, while there is no significant change in the proportions of black phase during this period. The initial appearance of the white phase coincided with the change in the electrical properties. However, the experiments conducted on specimen Ala indicated that the electrical resistivity and Seebeck coefficient can be further altered by subjecting the material to a further low temperature heat treatment although the white phase remains unchanged.

(iii) Scattering Mechanisms

(a) Introduction

The thermoelectric transport properties which occur in the figure of merit are dependent on the mechanisms which scatter the charge carriers. It has been speculated that the relative contributions of the scattering mechanisms operating in these alloys may change after heat treatment and this may be a contributing factor in enhancing the electrical power factor. One way of investigating the scattering mechanism is through the temperature dependence of the carrier mobility. This method was employed in the following investigation.

(b) Measurements

The Seebeck coefficient and electrical resistivity of the SiGe-GaP material was measured as a function of temperature over the temperature range 300-800K using the apparatus described in section 5b.

(c) Results

It was assumed that over the range of temperature the carrier concentration remained essentially constant. This is a reasonable assumption as no further ionisation of dopant occurs and measurements were made well below the intrinsic temperature. Hall effect data on SiGe alloys over the same temperature range support this assumption (16). Supportive evidence is also obtained by plotting the Seebeck coefficient against $\ln T$ (17). In Figure 19 the plots are straight lines which confirm that to a first approximation the carrier concentration remains constant with temperature. The carrier mobility μ in a semiconductor is related to the electrical conductivity σ by $\sigma = ne\mu$. If the carrier concentration remains constant, the temperature variation of the electrical conductivity represents the variation of the mobility. The mobility of the charge carriers can be assumed to vary with temperature according to $\mu \propto T^q$ where q is determined by the scattering mechanism. In this case, if the experimental data is displayed as $\ln \sigma$ against $\ln T$, the slope of the straight line dependence is the temperature dependence of the mobility. The dependences for SiGe-GaP alloys before and after heat-treatment are displayed in Figure 20. It is apparent that the slopes are slightly curved. This indicates that the parameters l and hence the electron scattering mechanism changes slowly with temperature. The temperature dependence of the mobility tabulated in Table 3 is obtained from the tangents to the curves at the temperatures indicated.

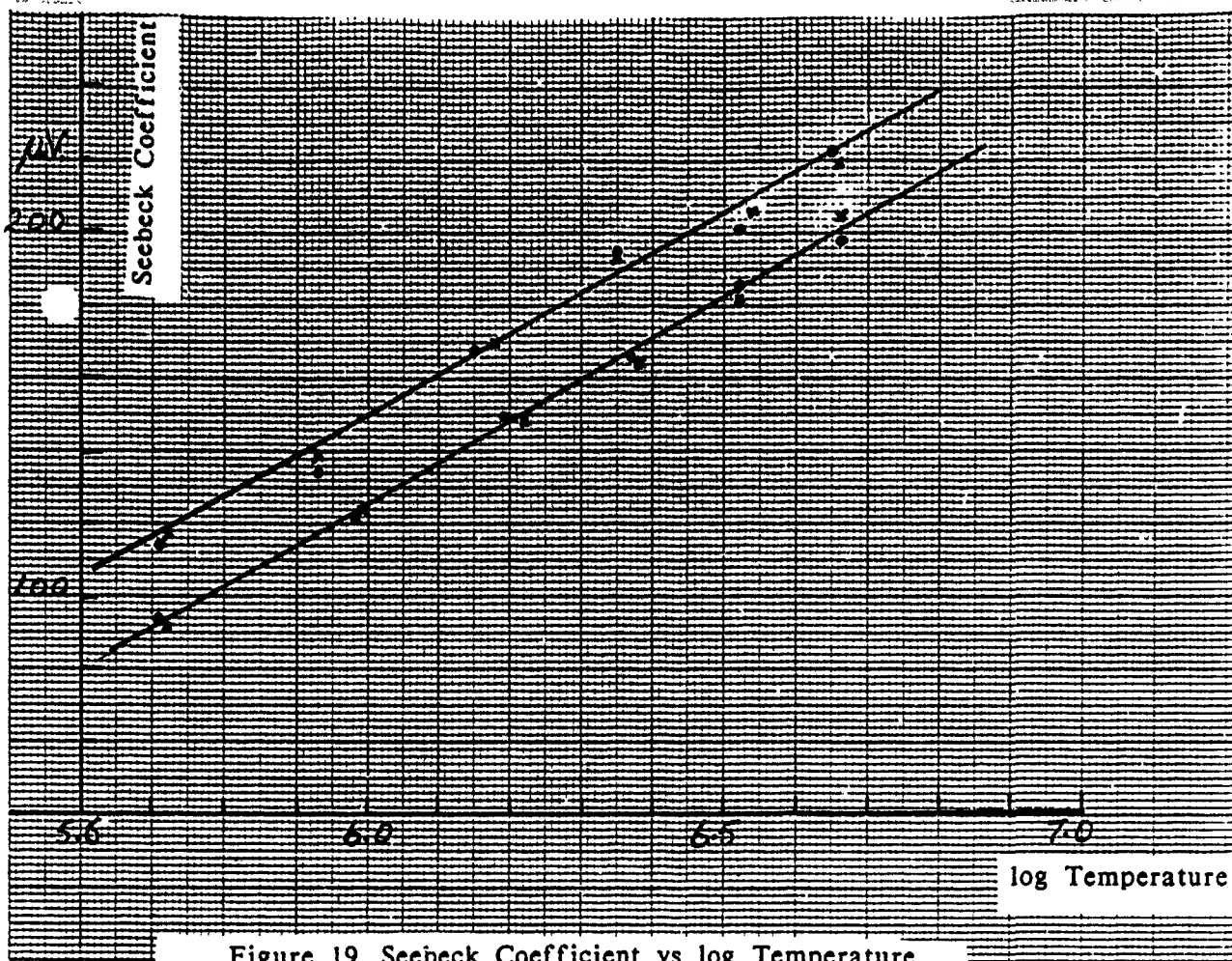


Figure 19 Seebeck Coefficient vs log Temperature

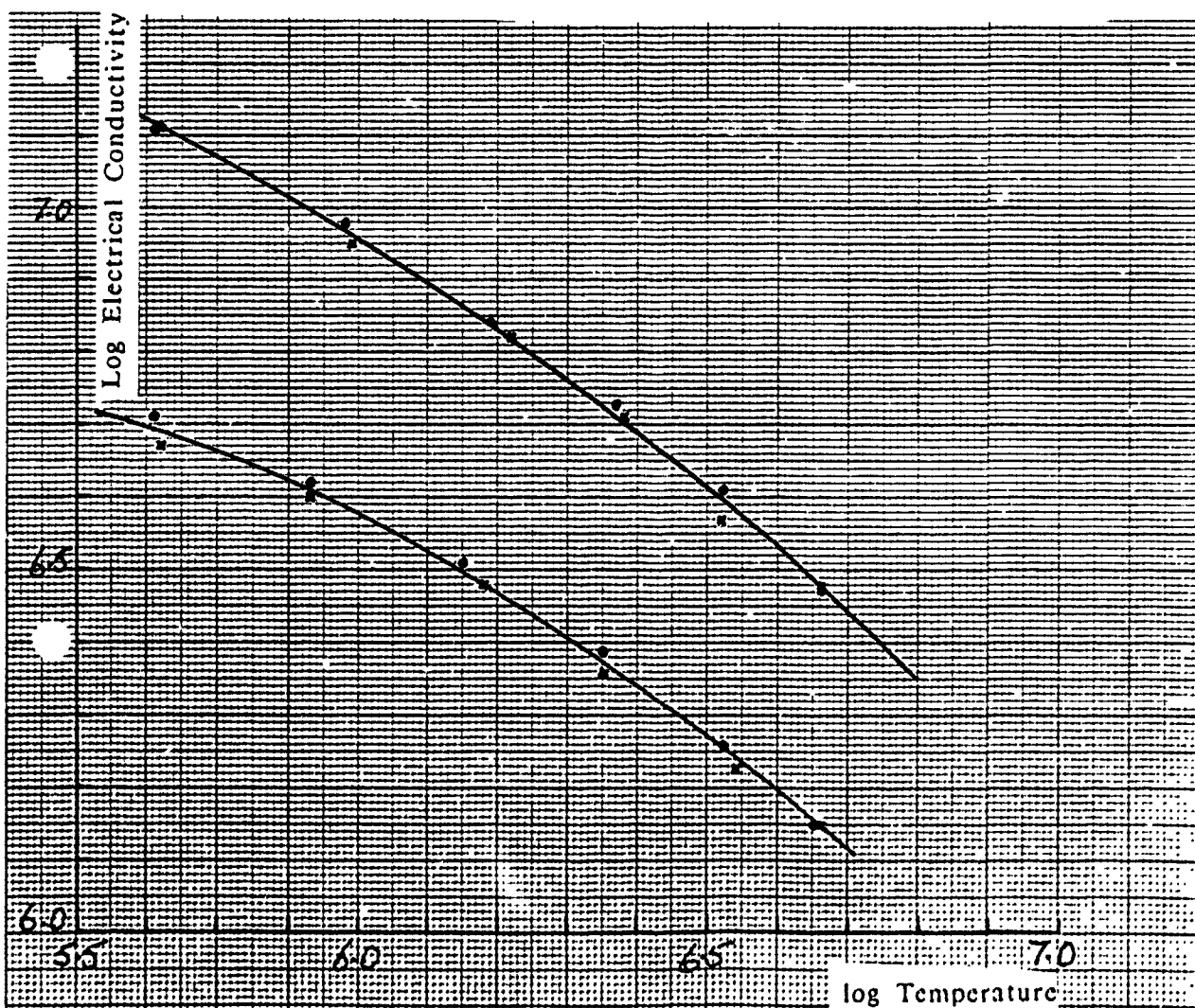


Figure 20 Log Electrical Conductivity vs log Temperature

TABLE 3

VALUES OF THE SCATTERING PARAMETER (q)

	<u>Before Heat Treatment</u>	<u>After Heat Treatment</u>
Room Temperature	-0.44	-0.60
800K	-0.73	-0.82

(d) Discussion

The SiGe-GaP alloys investigated are heavily doped. The electron scattering mechanisms in operation are: phonon scattering, $q = -3/2$; Point defect scattering $q = -1/2$ and ionised impurity scattering $q = 3/2$ with the relative importance each scattering mechanism strongly dependent on the temperature range. As the phonon-electron scattering increases with increase in temperature it is expected that the parameter q will become more negative with increase in temperature. This is supported by the tabulated data. In its simplest form the Seebeck coefficient can be expressed as

$$\alpha = k/e((5+q)/2 + \ln(N_c/n)) \quad \text{_____} \quad 1$$

where k is Boltzmann constant; e the electron charge; N_c the density of states, and n the charge carrier concentration. It is apparent that although the Seebeck coefficient decreases with an increase in the charge carrier concentration, this reduction could be offset by an increase in the parameter q , i.e. the electron scattering mechanism becomes more impurity scattering dominated. It is therefore speculated that the relatively small reduction in the Seebeck coefficient could be due in part to an increase in ionised impurity scattering. However, the experimental results indicate that contrary to expected phonon-electron scattering increases after high temperature heat treatment. This indicates that the change in the electron scattering mechanism cannot compensate for a reduction due to an increase in carrier concentration. Rather, it will reduce the Seebeck coefficient by about $10\mu\text{V/K}$. In searching for a possible explanation a

more general expression for the Seebeck coefficient was examined.

$$\alpha = \frac{k}{e} \left[\frac{1}{kT} \frac{F_2}{F_1} - \eta \right] + \frac{m^*}{T} f v_s^2 \left[\frac{\tau}{\tau_e} \right] \quad \text{--- 2}$$

$$\text{where } F = \frac{16 \sqrt{\pi(m^*)^{1/2}}}{3 h^3} \int_0^\infty Z_c(E) E^{n+1/2} \frac{-\partial f_0(\eta)}{\partial E} dE; \quad \eta = \frac{E_F}{kT} \quad \text{--- 3}$$

F is the Fermi integral, η the reduced Fermi level, T the absolute temperature, v_s the velocity of sound, m^* the effective mass, f the fraction of momentum transferred due to phonon-electron interaction, τ_e the relaxation time of phonon-electron interaction, τ the relaxation time associated with the Umklapp processes between the long wavelength and short wavelength phonons.

The first term in equation (2) is the familiar expression which represents the carrier diffusion contribution to the Seebeck coefficient; it is only dependent on the Fermi level and the scattering mechanisms. The theoretical calculation indicate that both increase in carrier concentration and in phonon-electron scattering dominance will result in a decrease in the Seebeck coefficient similar to the non-degenerate theory prediction (18). The second term is the so called phonon-drag contribution, which could increase with increasing the strength of the phonon-electron scattering (19). This may be a possible mechanism which can explain the insignificant reduction in the Seebeck coefficient with increase in carrier concentration and the dominance of phonon-electron scattering. In the first place the phonon-drag contribution to the Seebeck coefficient will increase with increasing f , i.e. the strength of the phonon-electron scattering. The above experimental results and the results of the thermal conductivity measurements (20) have shown a relative increase in the phonon-electron scattering after high temperature heat treatments. Therefore, if the effective mass m^* remains constant, the increase in f might result in an increase in the second term of the equation (2). Secondly, a large ratio τ/τ_e leads to a large phonon-drag effect, τ_e is obviously reduced to some extent by the increase in the phonon-electron scattering. If the Umklapp processes between the long wavelength phonons and short wavelength phonons remain constant, or preferably weakened by the high temperature heat treatment, then the phonon-drag contribution can be decreased further

as a result of the increase in the ratio τ/τ_e . It has been argued that the phonon-drag effect could be significant even at high temperature (21). Unfortunately, there is no direct experimental results present to support this argument, so that the above discussion remains a speculation. However, a more detailed understanding of the phonon-drag contribution to the Seebeck coefficient may provide a mechanism by which the Seebeck coefficient can increase while the electrical and thermal conductivity remain unchanged.

(iv) Long Term Stability

(a) Introduction

Long term stability is a very important requirement for materials used in space applications. It has been confirmed that the improvement in the thermoelectric properties of silicon germanium-gallium phosphide alloys is mainly due to a significant increase in the electrical power factor. However, no information has been reported relating to the long term stability of these materials under high temperature device operating conditions.

(b) Measurements

The specimens used were Ala and Alb. Following the established procedure employed in enhancing the power factor the specimens were heat treated in air at 1473K for 16 hours. Specimen Ala was subjected to a long term heat treatment at 973K and specimen Alb at 1273K for a period up to 4000 hours. The heat treatments were periodically interrupted by cooling the specimens to room temperature and measuring the Seebeck coefficient and electrical conductivity from room temperature to 800K.

(c) Results

The electrical power factor was calculated and is displayed as a function of heat treatment temperature in Figures 21 and 22. The data displayed

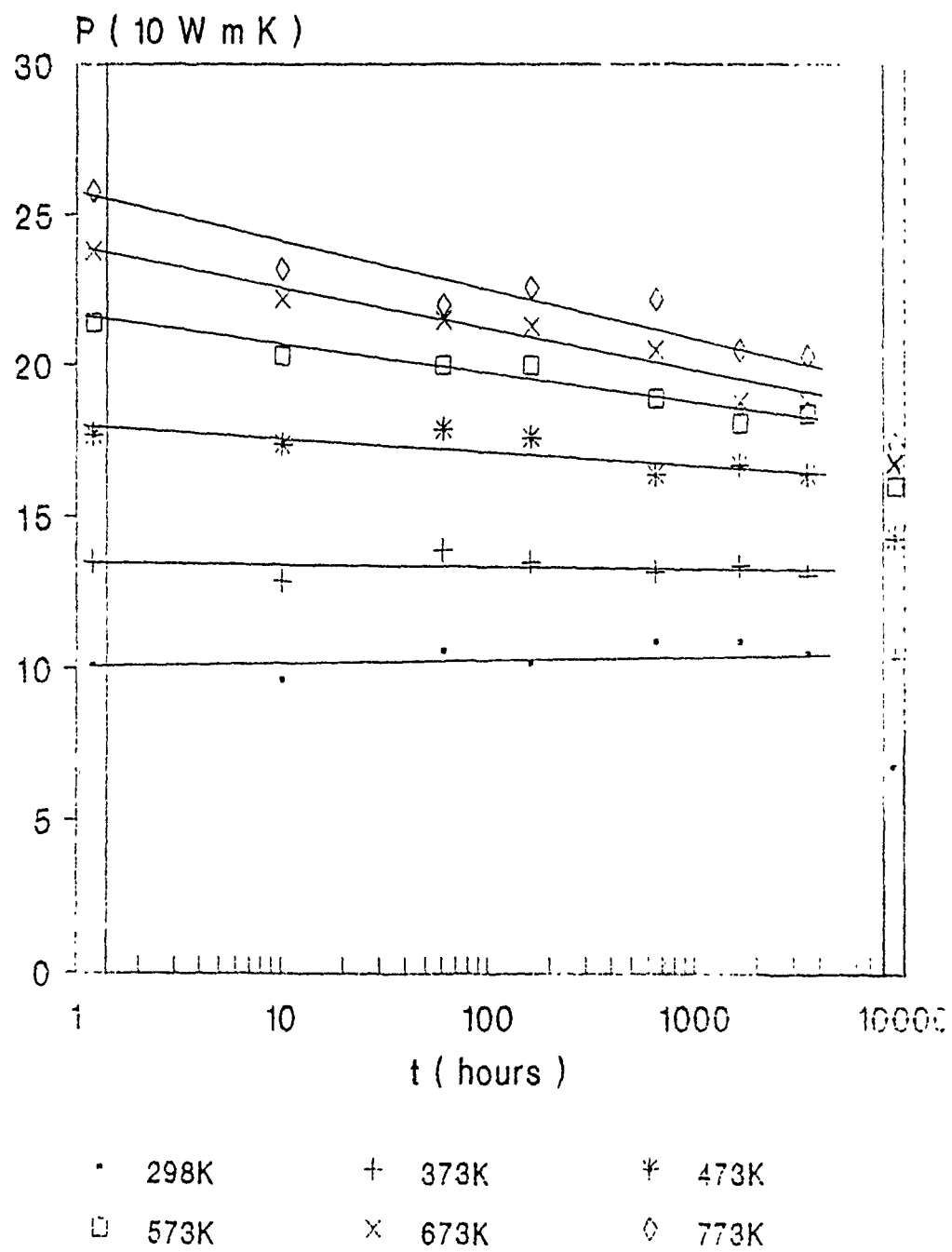


Figure 21 Power factor vs time specimen at 973K

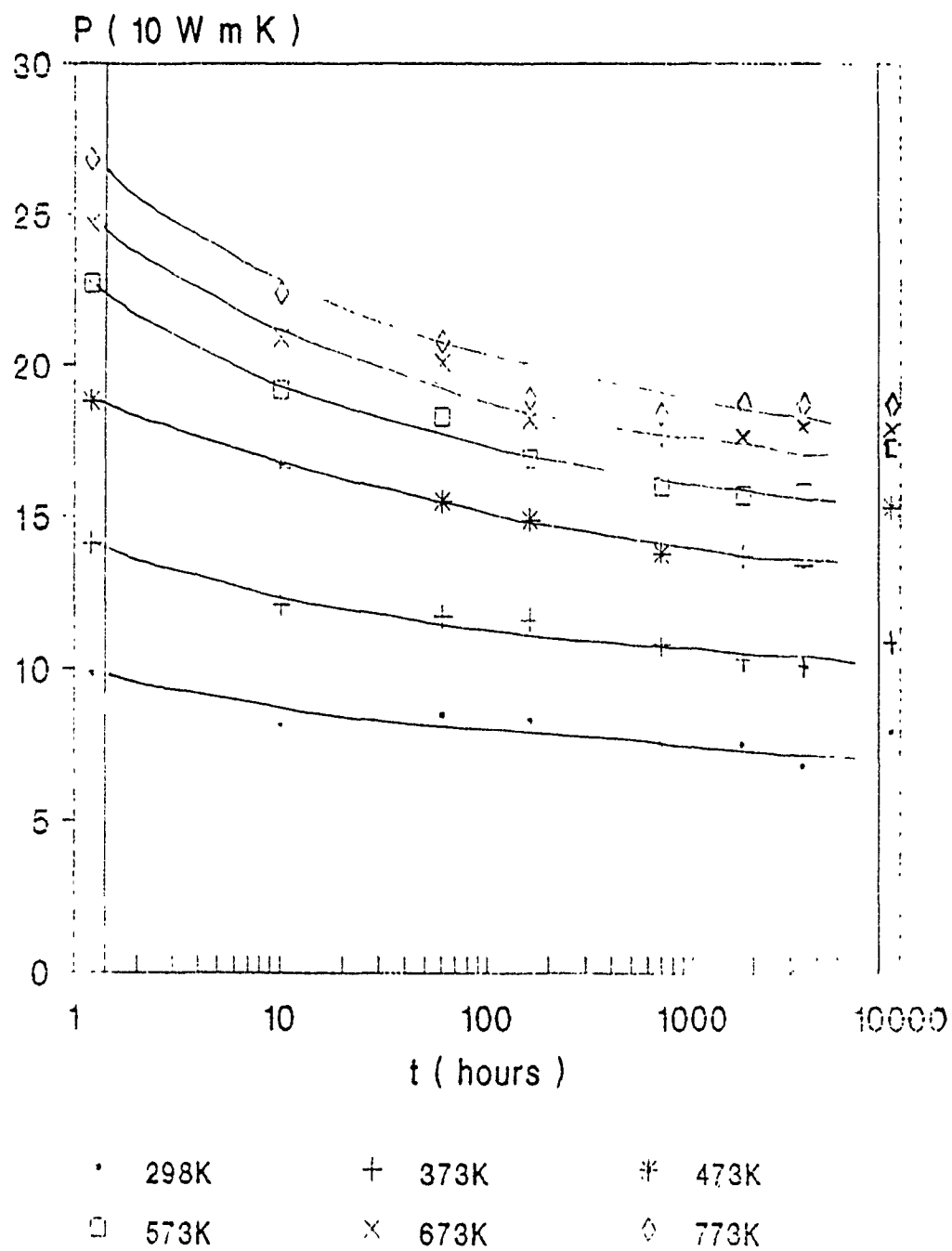


Figure 22 Power factor vs time; specimen at 1273K

on the right side column of the graphs are electrical power factors of "as grown" specimens. The data displayed in the left side column are the electrical power factors of the specimens after the first heat treatment at 1473K to improve their thermoelectric properties.

(d) Discussion

Evidently the electrical power factor of both specimens are significantly improved by this heat treatment. However, the power factor of both specimens decreases during heat treatment at lower temperatures. The decrease appears more significant in the specimen heat treated at the higher temperature. After 4000 hours heat treatment at 1273 the power factor of specimen Alb dropped to the original value of the as prepared material. The electrical power factor measured at room temperature and at 473K remains almost unchanged after the same period of heat treatment. The variation of the Seebeck coefficient with time of heat treatment and of the electrical resistivity with the log of heat treatment period exhibits a set of parallel at different temperature of measurement. This indicates that a decrease in carrier concentration may be responsible for the loss of initial enhancement in power factor - possibly due to precipitation of dopant as has been observed in silicon germanium alloys (22).

8 Conclusion

The work presented in this report embodies a number of significant results. It has been confirmed that improvements in the electrical power factor of silicon germanium-gallium phosphide accompanies high temperature thermal annealing. It has also been confirmed that this increase can be further increased by subjecting the material to a high-low-high temperature heat-treatment sequence. The results also show that the relative contribution of electronic and lattice component to thermal conductivity of silicon-germanium-gallium phosphide alloy is changed by cyclic high temperature heat treatment, although the total thermal conductivity remains approximately constant. An increase in the ratio λ_e/λ_L after heat treatment is beneficial to an improvement in the thermoelectric figure of merit of these materials. The increase in λ_e is due to a significant increase in the electrical conductivity, while a reduction in λ_L can be explained by an increase in the phonon-electron scattering, changes in

microstructure and alloy composition.

Although considerable effort was made to relate changes in the electrical properties with the material's morphology obtaining a correlation proved elusive. However, the highest power factor obtained in this investigation corresponded to a morphology which consisted of the host matrix and a significant proportion of white phase.

The investigation into the effect of high temperature heat treatment on the scattering mechanisms provided a surprise. The results provided evidence that the electron scattering mechanism in these alloys was altered after heat treatment; the temperature dependence of the mobility indicating that the electron-phonon scattering became stronger.

Finally the work on the long term stability of the electrical power factor revealed that the enhancement which accompanies high temperature heat treatment is unstable at device operating temperatures. The reported improvement in the thermoelectric figure of merit being almost totally lost after a relatively short period of heat treatment in air at operating temperatures.

9 Acknowledgements

Dr. Gao Min (on leave from Kunming Institute of Physics, China) is acknowledged for carrying out the majority of the measurements reported in this report and for his considerable input to the programme as a whole. Dr. C.M. Bhandari (University of Allahabad, India) is thanked for his valuable advice on various aspects of the work and Drs C. Wood and J.W. Vandersande (Jet Propulsion Laboratory, California, USA) for providing the Silicon Germanium-Gallium Phosphide material. Finally the United States Army European Research Office is acknowledged for supporting this research project.

References

1. Rowe, D.M., Shukla, V.S. and Savvides, N., 1981, Nature, Vol.290, No.5809, p765.
2. Pisharody, R.K. and Garvey, C.P., 1978, Proc. 13th IECEC, San Diego, Cal. p1963.
3. Vandersande, J.W., Wood, C. and Draper, S., 1987, Proc. Spring Meeting Mat. Res. Soc., Anaheim, Cal. p21.
4. Shukla, V.S. and Rowe, D.M., Applied Energy, Vol.9, 1981, p131.
5. Shukla, V.S. and Rowe, D.M. Physica Status Solidi, Vol.66, No.1, 1981, P243.
6. Justice, W.H., 1987, Final Year BSc Project, University of Wales Cardiff.
7. Powell, R.W., Jenkins, R.J., 1962 Prog. in Int. Res. on Thermodynamic and Transport Properties - 2nd Symposium ASME, Princeton, N.J., p454.
8. Touloukian, Y.S et al, Thermophysical Properties of Matter, 1973, Vol.10 Thermal Diffusivity, New York, IFI/Pleum.
9. Rowe, D.M. and Min Gao, 1990, J.Appl.Phys., 23, p258.
10. Valdes, L.B., 1954, Proc. IRE, 42, p420.
11. Cowles, L.E. and Dauncey, L.A., J.Sci. Instrum. Vol.39, p1.
12. Rowe, D.M. and Bhandari, C.M. 1983, Modern Thermoelectrics (Holt, Rinehart and Winston, London) p258.
13. Dismukes et al, 1964, J.,Appl. Phys. 35, p2899.
14. Parrott, J.E., 1989, Proc. 8th Int. Conf. on Thermoelectric Energy Conversion, Nancy, France, p185.
15. Abeles, B., 1963, Phys. Rev. 131, p1906.
16. Rowe, D.M. 1975, Journal Phys.D.Appl.Phys. Vol.8, p1092.
17. Goldsmid, H.J., 1957, Ph.D. Thesis, University of London.
18. Bhandari, C.M. and Rowe, D.M., 1988, Thermal Conduction in Semiconductors, Wiley Eastern.
19. Herring, C., 1954, Phys. Rev. 96, p1163.
20. Rowe et al. To be published
21. Ure, R.W. and Heikes, R.R., 1961, "Thermoelectricity"; Science and Engineering (London; Interscience)
22. Savvides, N. and Rowe, D.M., 1981, J.Phys. D., Appl. Phys., Vol.24, p723-32.